Dryland Soil Research, Vol. 1, No. 2, pp. 43-57, 2025
Type of article: Original, Available online at www.dlsr.iut.ac.ir,
https://doi.org/10.47176/dlsr.01.02.1033

Integration of Remote and Proximal Sensing Techniques for Soil Salinity Assessment of Pistachio Orchards

Yousef Hasheminejhad[1†] and Hossein Beyrami[2]

[1] *Khorasan Razavi Agricultural and Natural Resources Research and Education Center, Agricultural Research, Education and Extension Organization (AREEO), Mashhad, Iran*
[2] *National Salinity Research Center, Agricultural Research, Education and Extension Organization (AREEO), Yazd, Iran*

†*Corresponding Author Email: hasheminejhad@gmail.com*

(Received 11 March 2025, Accepted 04 May 2025)

ABSTRACT

Soil salinity is a property that varies in space and time. In pistachio orchards irrigated with saline and brackish water sources, understanding the variability of soil salinity is crucial for managing irrigation and leaching practices. Excessive leaching leads to water loss, while insufficient leaching results in salt accumulation in the soil, ultimately reducing water productivity. Traditional methods of assessing soil salinity, which rely on sampling and laboratory analysis, are both time-consuming and costly for understanding this temporal and spatial variability. Utilysing the remote and proximal sensing tools can reduce the time and cost of monitoring soil salinity changes. This project was designed and executed to evaluate these methods in mapping soil salinity variations in the field and for local scales. The proximal sensing indicators in this study included measuring the apparent electrical conductivity of the soil using the EM38 device, as well as measuring the canopy diameter and the number of clusters on pistachio trees. Remote sensing indicators included the mean digital numbers of Sentinel-2 satellite sensors and vegetation indices derived from them. Ground measurements involved soil sampling from 25 points in a 75-hectare pistachio orchard in Khorasan Razavi Province, down to a depth of 90 cm at 30 cm intervals. Results showed that models using RS and PS indicators, both individually and in combination, could predict soil salinity with statistically significant relationships ($P < 0.01$). However, the determination coefficients (R^2) were relatively low, ranging from 0.26 to 0.56, indicating moderate predictive power. Among the methods tested, the Partial Least Squares Regression (PLSR) model based on remote sensing variables was applied to predict salinity over a larger 4080-hectare area using a combination of Google Earth Engine and R coding media. The Support Vector Machine (SVM) model yielded the highest mapping accuracy for interpolation (R^2 = 0.9, RMSE = 0.75 dS/m), demonstrating its relative effectiveness in spatially predicting soil salinity.

Keywords: Pistachio, Satellite imagery, Soil Salinity, Remote sensing, Proximal sensing, Machine learning.

1. Introduction

Soil salinization occurs due to two main factors: natural processes (primary salinization) and human-induced activities (secondary salinization). These processes negatively affect soil quality, crop yields, hydrology, geochemistry, and socio-economic conditions (Albed and Kumar, 2013). Severe salinity can lead to long-term challenges, including salt dust storms, poverty, migration, and expensive soil rehabilitation efforts (Hassani et al., 2020).

In irrigated agricultural lands of Iran, with free natural drainage, the most significant cause of soil salinization is the use of highly saline water for irrigation and poor irrigation management, which are classified under secondary salinization factors.

Most pistachio orchards are irrigated using brackish, saline, or highly saline water, making soil salinity control in the root zone even more critical (Rahimian et al., 2019). Repeated soil salinity measurements are needed to assure if the leaching is sufficient for maintaining sustainable production. However, frequent laboratory measurements of soil salinity across large areas, if not impossible can be both time-consuming and costly. With the advancement of technology, various tools for proximal sensing (like EM38) and improvement of remote sensors have created new opportunities to speed up such assessments and reduce their costs.

Projections suggest that by 2050, over 50% of the world's arable land could become saline (Muhetaer et al., 2022). The extent and rate of salinity increase vary globally, with the most severely impacted regions found in Asia, particularly China, Kazakhstan, and Iran, as well as parts of Africa and Australia (Hassani et al., 2020; Gao et al., 2022). However, due to the complex and dynamic nature of soil salinity, these estimates are largely empirical, making it difficult to generate a reliable global inventory (Scudiero et al., 2014). In Iran, various estimates suggest that 30% to 50% of the country's land area is affected by saline and sodic soils (Ghasemi et al., 1995; Khorsandi et al., 2010; Moameni, 2010).

Traditional methods of assessing soil salinity rely on time-consuming and expensive laboratory analyses. To

overcome these confines, alternative techniques, such as geostatistics (Brunner et al., 2007), remote sensing (Fourati et al., 2017; Ren et al., 2019; Dong et al., 2019; Taghizadeh Mehrjardi et al., 2021), electromagnetic induction (Iyer, et al., 2014), portable X-ray fluorescence (PXRF) sensors (Yimer et al., 2022), and visible-near infrared spectroscopy (Vis-NIR) (Wang et al., 2018, 2023), have been applied to predict soil salinity in unsampled areas. The integration of digital soil mapping (DSM) with machine learning techniques has further expanded these applications (Peng et al., 2019).

Haq et al. (2023) employed five machine learning models combined with RS data to predict soil salinity in Pakistan, with the Random Forest model showing superior accuracy. Similarly, Xiao et al. (2023) tested three machine learning models—Random Forest, Support Vector Machine, and Extreme Gradient Boosting—for predicting soil salinity in northwest China. The Extreme Gradient Boosting model outperformed the others, highlighting the importance of selecting the right model based on input data.

In northern Xinjiang, China, Zhao et al. (2024) combined Partial Least Squares (PLS) Vis-NIR spectroscopy and RS data to predict Electrical Conductivity (EC) and Sodium Adsorption Ratio (SAR). Their results showed that combining Vis-NIR data with topographical features and Random Forest models produced reliable predictions, offering insights for identifying high-risk salinity areas and informing management practices to mitigate degradation.

In a feasibility study, Zare et al. (2021) assessed three methods—visible and near-infrared diffuse reflectance spectroscopy (VisNIR DRS), portable X-ray fluorescence spectroscopy (PXRF), and remote sensing (RS)—to predict soil salinity in Texas salt flats. They found that combining these three techniques significantly improved predictive accuracy compared to individual methods, making it a promising approach for rapid salinity assessment.

Digital soil mapping accuracy is often constrained by the limited availability of soil data. However, studies have shown that increasing the spatial density of soil sampling improves DSM model performance (Lagacherie et al., 2021). Soil sensing technologies, including remote sensing and proximal soil sensing, offer an alternative to direct soil measurements, providing denser spatial data under certain conditions.

Several technologies, including VIS-NIR-SWIR spectroscopy, gamma spectroscopy, ground-penetrating radar, and airborne hyperspectral imagery, have been successfully used to estimate soil properties. Among these, electromagnetic induction (EMI) has gained popularity for mapping soil properties that influence electrical conductivity, such as clay content, moisture, and pH, making it particularly valuable for soil salinity monitoring (Taghizadeh Mehrjardi et al., 2016).

Most studies using soil sensing as a sole data source have not integrated it with prior knowledge of soil distribution. However, incorporating soil sensing data into digital soil mapping could enhance the accuracy of soil property maps. Methods such as regression Kriging and random forest algorithms have been used to integrate EMI and environmental variables, resulting in improved soil salinity assessments (Wang et al., 2021).

Wang et al. (2024) proposed a new framework that integrates data from Sentinel-1 and Sentinel-2 satellites with climate, topography, and machine learning techniques to estimate soil salinity at a 10-meter resolution. Field validation in Iran and Xinjiang demonstrated significant accuracy improvements compared to previous salinity maps, offering a high-quality foundation for soil property studies.

Remote sensing (RS) has become increasingly important in evaluating soil salinity, with satellite sensors offering higher temporal resolution and improved spatial and spectral imagery. Platforms such as Google Earth Engine (GEE) facilitate access to and analysis of satellite images, enabling the creation of specialized products like soil salinity change maps. For satellite-derived data analysis, various machine learning (ML) methods have been developed in both online systems and coding environments, making it easier to explore complex relationships between soil salinity and environmental variables. Spatial modeling methods also allow for the evaluation of models suited for salinity assessment, helping identify the most appropriate approaches for specific conditions. This research explores the hypothesis that combining remote sensing, proximal sensing, and spatial modeling techniques can produce a reliable model for assessing salinity in pistachio orchards.

Some limitations remain while trying to predict soil salinity in pistachio orchards using remote and proximal sensing. First, despite referencing several studies on salinity mapping, questions still persist regarding the transferability of models developed at the orchard scale to larger regional extents. Additionally, many referenced works emphasize salinity detection under uniform or bare soil conditions, whereas this study dealt with complex, vegetated orchard systems, where canopy structure may obscure salinity signals.

While previous studies have explored soil salinity mapping using either remote sensing or proximal sensing techniques independently, this study is among the few that integrates both approaches in pistachio orchards, which are often irrigated with brackish water. The research not only evaluates the individual and combined predictive power of EM38 measurements and Sentinel-2 derived indices but also scales up the results using the Google Earth Engine (GEE) and machine learning algorithms to map soil salinity over a large area (4080 ha). The integration of proximal sensing data, canopy indicators, and satellite imagery into a unified machine learning framework, and its operational application via GEE, provides a practical and scalable model for precision

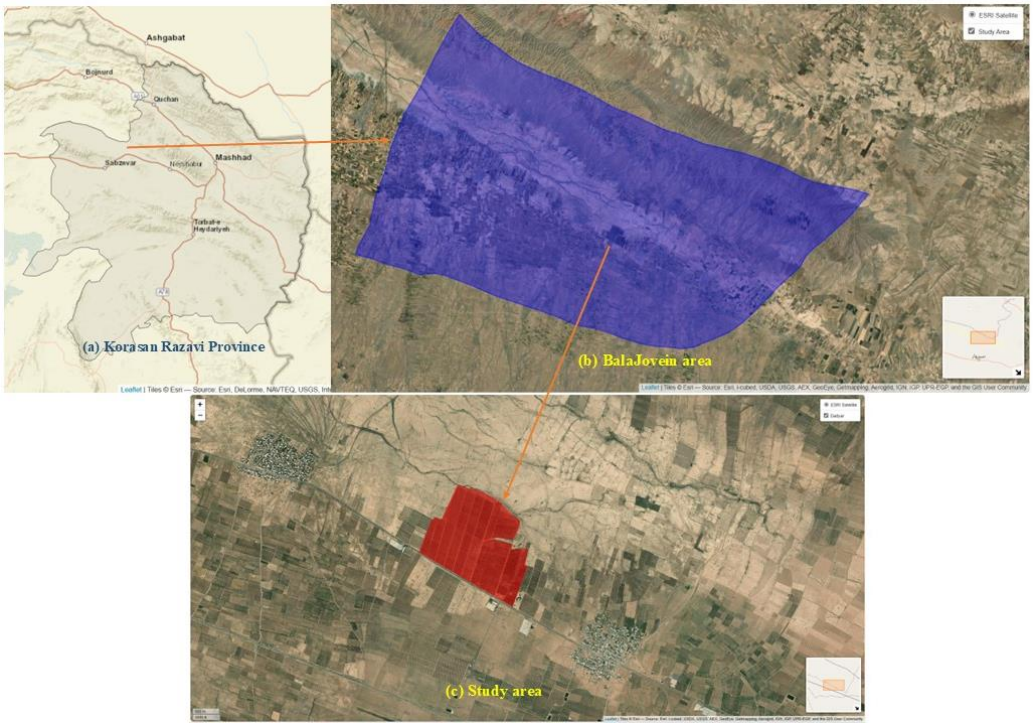

Figure 1. The study area location, Khorasan Razavi Province (a), Baala Jovein County (b) the field area (c).

salinity management in perennial tree crops. This combined approach, specifically validated in pistachio systems of Iran, represents a novel methodology with high relevance for sustainable salinity monitoring and decision-making.

The main objectives of this study were:

(1) To evaluate the effectiveness of remote sensing (Sentinel-2) and proximal sensing (EM38, canopy diameter, and cluster count) indicators in predicting soil salinity in pistachio orchards irrigated with saline water;

(2) To develop and compare statistical and machine learning models (e.g., PLSR and SVM) for soil salinity prediction using individual and combined data sources;

(3) To apply the most accurate model for large-scale salinity mapping (over 4080 ha) using Google Earth Engine (GEE) integrated with R programming.

2. Materials and Methods

For the implementation of this project, ground data was collected from a commercial pistachio orchard with an approximate area of 100 hectares in Jovein County, Razavi Khorasan Province (36:25-36:50 N and 57:12-5730 E). Figure 1 shows the location of this orchard in Razavi Khorasan Province. The ground data included soil sampling, down to a depth of 90 cm at intervals of 30 cm, at 25 points (a total of 75 samples). The proximal-sensing variables measured included the apparent soil electrical conductivity using the EM38 device at all 75 points in summer, counting the number of clusters (75 trees), and measuring the canopy diameters (of 75 trees). Remote sensing variables included the digital number values of the Sentinel-2 sensor's reflective spectrum from bands 2 to 9, and the NDVI (Normalized Difference Vegetation Index) was calculated (NDVI = (NIR−Red)/(NIR+Red)) from Sentinel-2 images using the reflectance values from two specific spectral bands: the Red band (B4) and the Near-Infrared (NIR) band (B8). To retrieve the RS data, the values from April 1st to the end of September (year ??) were extracted and downloaded using the Google Earth Engine system.

After extracting the remote sensing values, the PLSR method was used to model the relationships between auxiliary variables and the measured soil salinity values, and to validate the results. The best resulting model was applied to generalize the results to a larger area.

To extend the results to a larger scale, land use types were first classified using machine learning algorithms available in the Google Earth Engine system, such as Random Forest and Support Vector Machine. Based on this classification, the boundaries of pistachio orchards in the county were extracted and matched with the ground truth. Then, using the same system, a sampling grid was designed over the entire orchards, from which the auxiliary variable values were determined for the desired points. The best model from the previous step was applied to the sampling points, and the soil salinity values were extracted at those points.

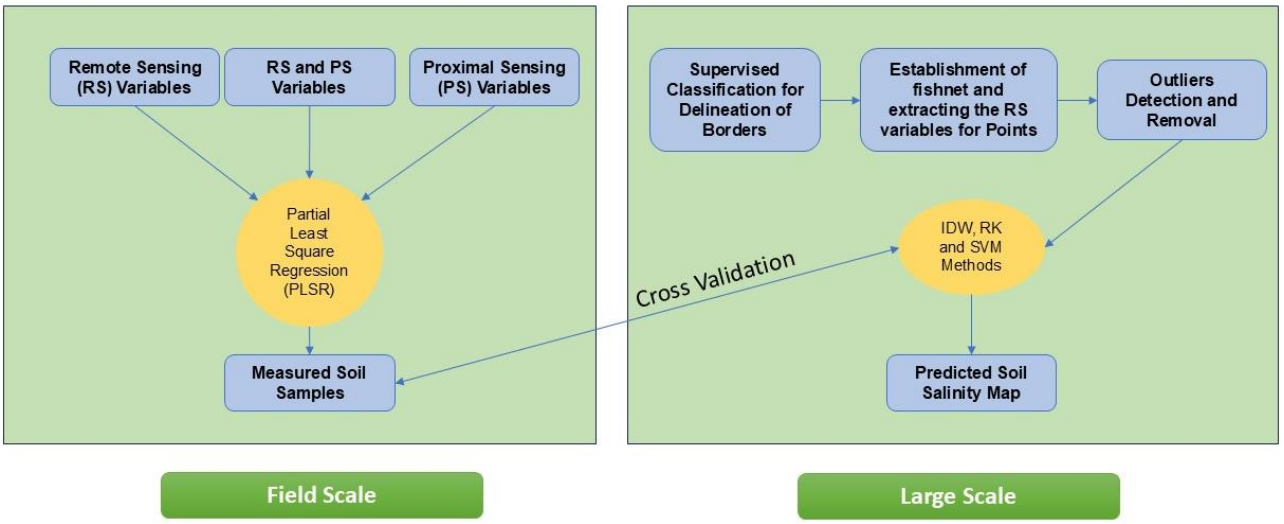

Figure 2. Flow chart illustration of methodology used in this research

Table 1. Analysis of Variance for PLSR of Proximal Sensing Data

Source	DF	SS	MS	F	P
Regression	3	124.290	62.1448	24.64	0.000
Residual Error	14	52.956	2.5217		
Total	17	177.246			

In the next step, outliers were identified and removed using the R scripts, and various interpolation methods such as Inverse Distance Weighting (IDW), Regression Kriging (RK), and Support Vector Machine (SVM) were applied to the remaining data. These methods were used to create soil salinity variation maps and validate the results. Figure 2 summarizes the methodology used in this research as a flow chart.

3. Results and Discussion

3.1. Estimation of Soil Salinity Using Only Proximal Sensing

The auxiliary variables from proximal sensing, including EM38 measurements, canopy diameter, and cluster count, provided a good estimation of soil salinity, which was significant at the 1% level. Table 1 shows the results of the analysis of variance for estimating soil salinity using proximal sensing data with the partial least squares regression method. Based on this table, the model used is significant at the 99% probability level.

Figure 3 shows the correlation between the mean values of measured electrical conductivity of the saturated extract and the estimated values from the partial least squares regression (PLSR). Although this regression is significant, in Minitab software, it is possible to re-evaluate the regression relationships using the leave-one-out (LOO) cross-validation (CV) method. In this method, one point is left out, and the regression model is developed for the remaining points, after which the left-out point is estimated using this model.

Figure 4 shows the relationship between the measured values and the cross-validation values. Based on this, the regression does not have enough power in unknown points and underestimates or overestimates soil salinity in about 65% of the cases.

Marino et al. (2019) reported in their assessment of pistachio evapotranspiration under saline-sodic conditions in California that since soil salinity significantly impacts pistachio photosynthetic properties and light absorption, these characteristics should be evaluated using remote and proximal sensing variables. Corwin and Scudiero (2019) concluded in a review that advances in proximal sensing tools, such as electromagnetic induction, have enabled soil salinity mapping from farm to regional scales.

3.2. Estimation of Soil Salinity Using Only Remote Sensing

The auxiliary variables derived from remote sensing alone could also estimate soil salinity well within the study areaand at a 1% significance level. Table 2 shows the analysis of variance for the partial least squares regression in this stage.

Figure 5 shows the linear regression between the measured soil salinity values and those estimated using

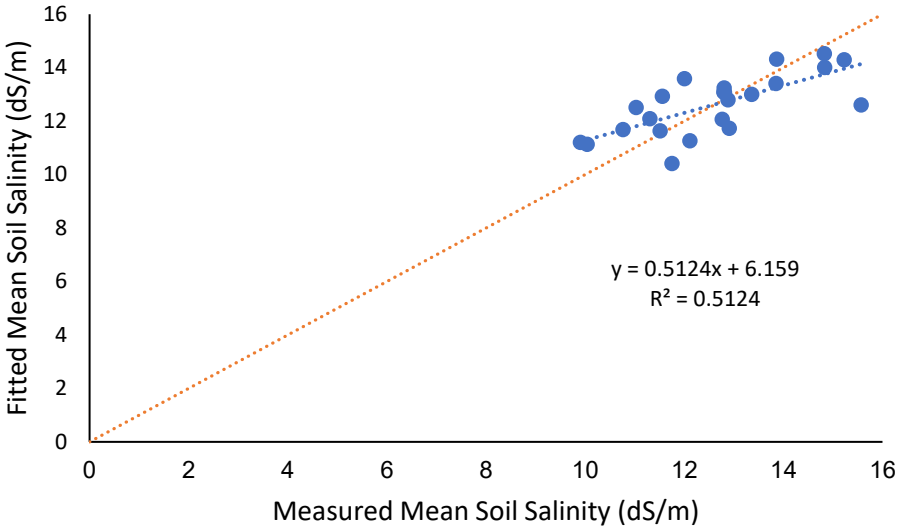

Figure 3. Regression between measured and estimated soil salinity values from proximal sensing

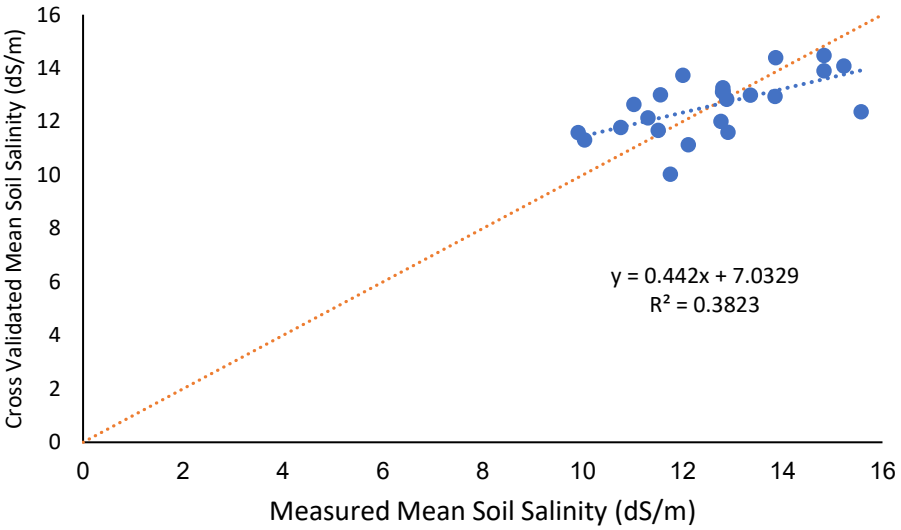

Figure 4. Regression between measured and cross-validation soil salinity values

Table 2. Analysis of variance for PLSR of remote sensing data

Source	DF	SS	MS	F	P
Regression	3	25.1540	8.38466	5.68	0.009
Residual Error	14	20.6629	1.47592		
Total	17	45.8169			

remote sensing auxiliary variables. This regression improved compared to using only proximal sensing data, but after cross-validation, the regression (Figure 6) became weaker than before.

Shamsi et al., (2022) reported that Sentinel-2 images combined with agro-hydrological models can be used to monitor soil salinity changes in pistachio orchards. By studying the time series of soil salinity changes using supervised and unsupervised classifications of satellite images around Lake Urmia, Delavar et al., (2020) found

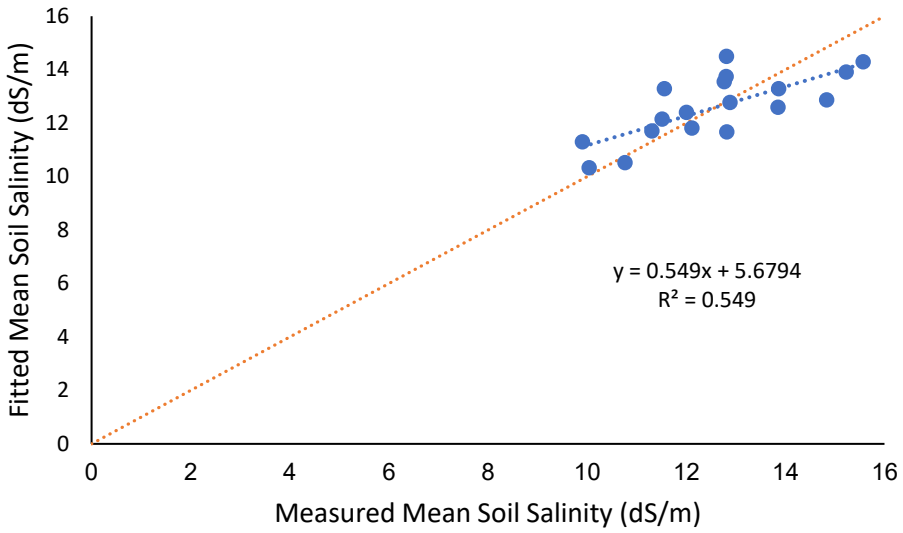

Figure 5. Regression between measured and estimated soil salinity values from remote sensing

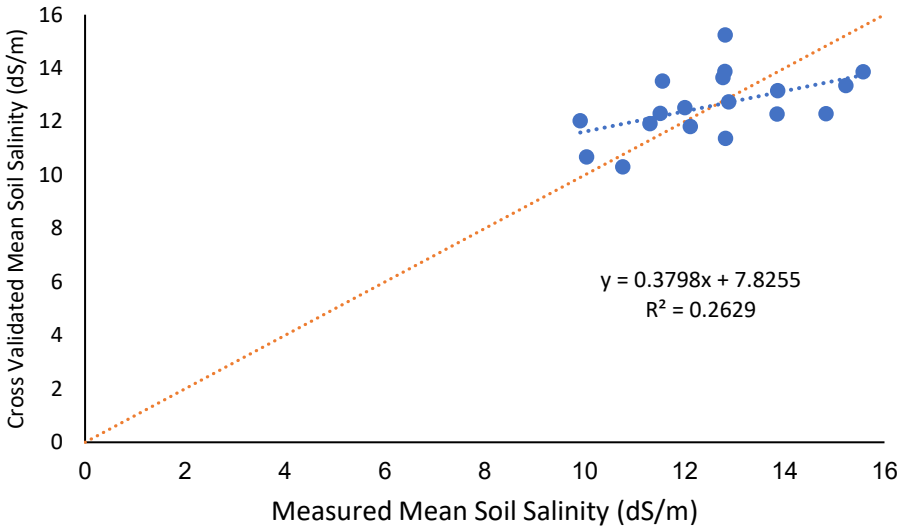

Figure 6. Regression between measured and cross-validation soil salinity values

that the extent of highly saline areas in the region increased over a research period of approximately 40 years.

3.3. Estimation of soil salinity using both remote and proximal sensing

In the next stage, soil salinity was estimated by integrating remote and proximal sensing data. Table 3 shows the analysis of variance for partial least squares regression to estimate soil salinity using both remote and proximal sensing data. Based on this table, the regression is significant at the 1% level.

Figure 7 shows the linear regression between the measured soil salinity values and the estimated values using the combined auxiliary variables from remote and proximal sensing. According to this figure, using both data sources improved the linear regression for estimating average soil salinity. However, this regression weakened in cross-validation (Figure 8).

Although the analyses of variance (tables 1-3) showed statistically significant relationships between actual and predicted EC values ($P < 0.01$), the coefficients of determination (R^2) were relatively low (Figures 3–8), indicating limited predictive power. These results suggest that while the models can capture broad spatial trends in soil salinity, they lack precision in estimating EC values at

Table 3. Analysis of variance for PLSR of combined remote and proximal sensing data

Source	DF	SS	MS	F	P
Regression	3	25.7365	8.57884	5.98	0.008
Residual Error	14	20.0804	1.43431		
Total	17	45.8169			

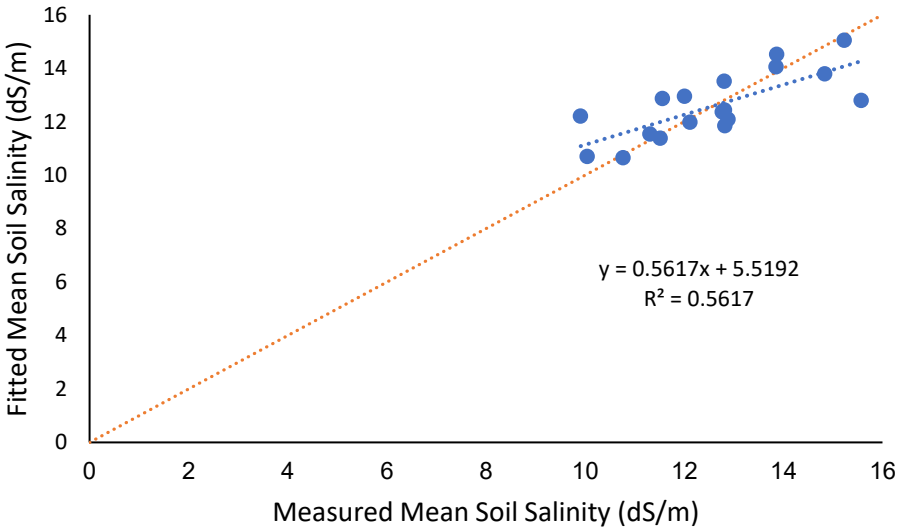

Figure 7. Regression between measured and estimated soil salinity values from remote and proximal sensing

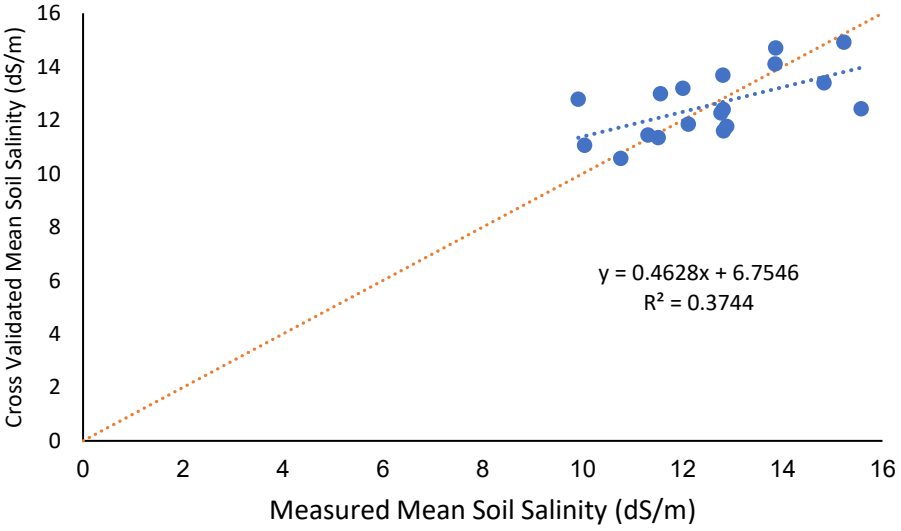

Figure 8. Regression between measured and cross-validation soil salinity values

finer scales. The low R^2 values likely reflect factors such as spatial variability within the orchard, measurement uncertainty, and the limited sensitivity of remote sensing variables to subtle salinity differences. Despite these limitations, the models were applied at a broader scale to explore potential salinity distribution patterns across the region. Therefore, the results should be interpreted with caution, recognizing that they provide a general overview rather than highly accurate point-level predictions. These limitations are consistent with prior findings that

Table 4. Confusion matrix for different land uses.

Land Cover	Barren	Pistachio	Urban	Fields	River	Classification accuracy (%)
Barren	29	2	0	2	2	83
Pistachio	0	36	0	4	0	90
Urban	0	0	18	1	1	90
Fields	2	6	1	26	3	68
River	7	0	5	2	9	39

RS-based salinity predictions often have reduced accuracy at fine spatial scales due to field variability, sensor sensitivity, and the indirect relationship between spectral signals and soil salinity (Allbed and Kumar, 2013).

According to the results, adding proximal sensing variables to remote sensing variables created a stronger linear regression. However, to generalize the method for mapping on a larger scale, proximal sensing data are either unavailable or difficult to measure and calculate. Therefore, for large-scale soil salinity mapping, the model should rely solely on remote sensing data.

Tavares et al. (2024) used the integration of remote sensing data and proximal sensing data from EM38 to map soil salinity at the farm scale in a semi-arid region of northeastern Brazil.

3.4. Large-Scale Soil Salinity Estimation

Before generalizing the model to a larger scale, the boundaries of the pistachio orchards in the study area needed to be determined. This is important because the regression model created for predicting soil salinity is only valid within the pistachio orchards. Therefore, remote sensing data should only be extracted for pistachio orchard areas for prediction purposes.

To this end, the Google Earth Engine (GEE) platform was used. In this platform, besides the specific codes for selecting and filtering satellite images and extracted products, special codes for classifying images exist, which, using machine learning algorithms like Random Forest and Support Vector Machine and inputting training points, can classify the area into defined land uses. The script developed specifically for this project with the help of generative AI, ChatGPT OpenAI, after classifying the area into different land uses and evaluating the classification accuracy, isolated the pistachio orchard boundaries from all land uses, removed areas less than 1000 square meters, and finally saved the created shapefile in Google Drive for further use. Figure 9 shows the boundaries of pistachio orchards in the Balajovein region of Jovein County delineated using this method.

The overall classification accuracy was 75.6%. This means that the method used was able to correctly identify land use in more than 75% of cases. The classification error matrix is presented in Table 4. According to this table, land use for pistachio and urban areas was estimated with 90% accuracy, but riverbeds were estimated with the lowest accuracy. In this project, the goal was to separate pistachio-cultivated lands, which was successfully achieved with good accuracy. The total area of pistachio-cultivated land in the study area was estimated at 4,080 hectares, which, compared to the official statistics reported by the county's agricultural management office of 4,300 hectares, had only about a 5% difference. Figure 10 shows that the script used correctly delineated the boundaries of the studied orchard.

In the next step, a regular grid of 200 by 200 meters was established over the study area. For the center points of this grid, values of auxiliary remote sensing variables were extracted and stored in a CSV file. Figure 11 shows the location of the sampling points in the study area.

Using three variables—residual error X, residual error Y, and leverage—the outliers were identified and removed.

Figure 12 shows a 3D plot of outlier detection using this method, with outliers marked in red. Also, Figure 13 shows the position of outliers on the sampling points distribution map.

After identifying and removing the outliers, the relationships between the auxiliary variables were examined. The highest correlation was observed between the estimated soil salinity and band values 2, 3, 4, and 5, and the average NDVI values for the months of April, May, August, and September. The correlation matrix between the variables is presented in Figure 14. Given the correlations between the auxiliary variables, partial least squares regression was deemed more suitable than stepwise regression for estimating soil salinity. Therefore, the partial least squares regression model extracted from the studied orchard was used to estimate soil salinity values at the sampling points.

The estimated soil salinity values obtained through partial least squares regression were then interpolated using various methods. Figures 15 to 17 show the interpolation maps created using IDW, RK, and SVM methods.

Table 5 shows the accuracy assessment of these three methods for generating the soil salinity map. Based on this assessment, the support vector machine method was identified as the most suitable for interpolation and creating the soil salinity map.

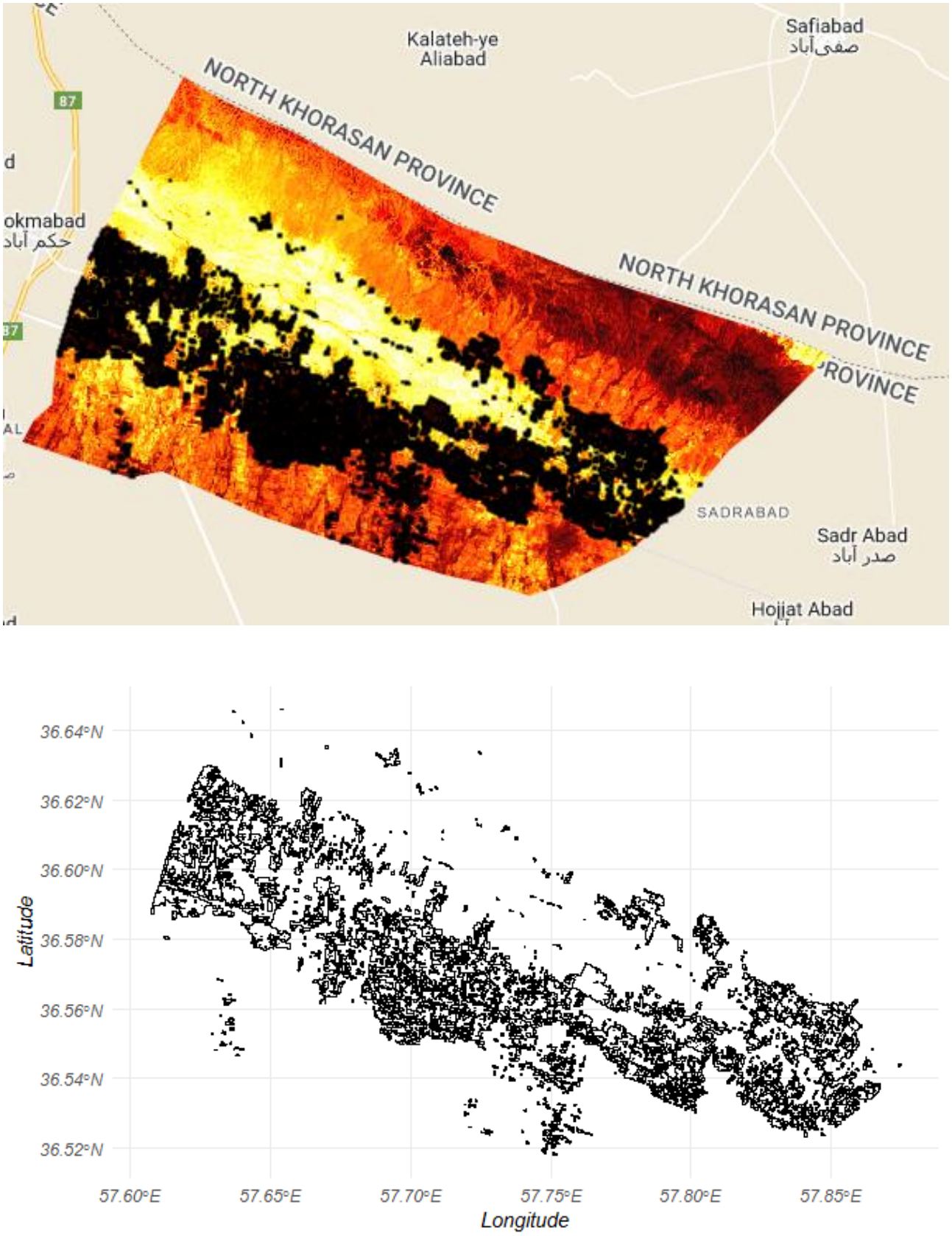

Figure 9. Pistachio orchard boundaries in Balajovein, Jovein County, delineated using GEE

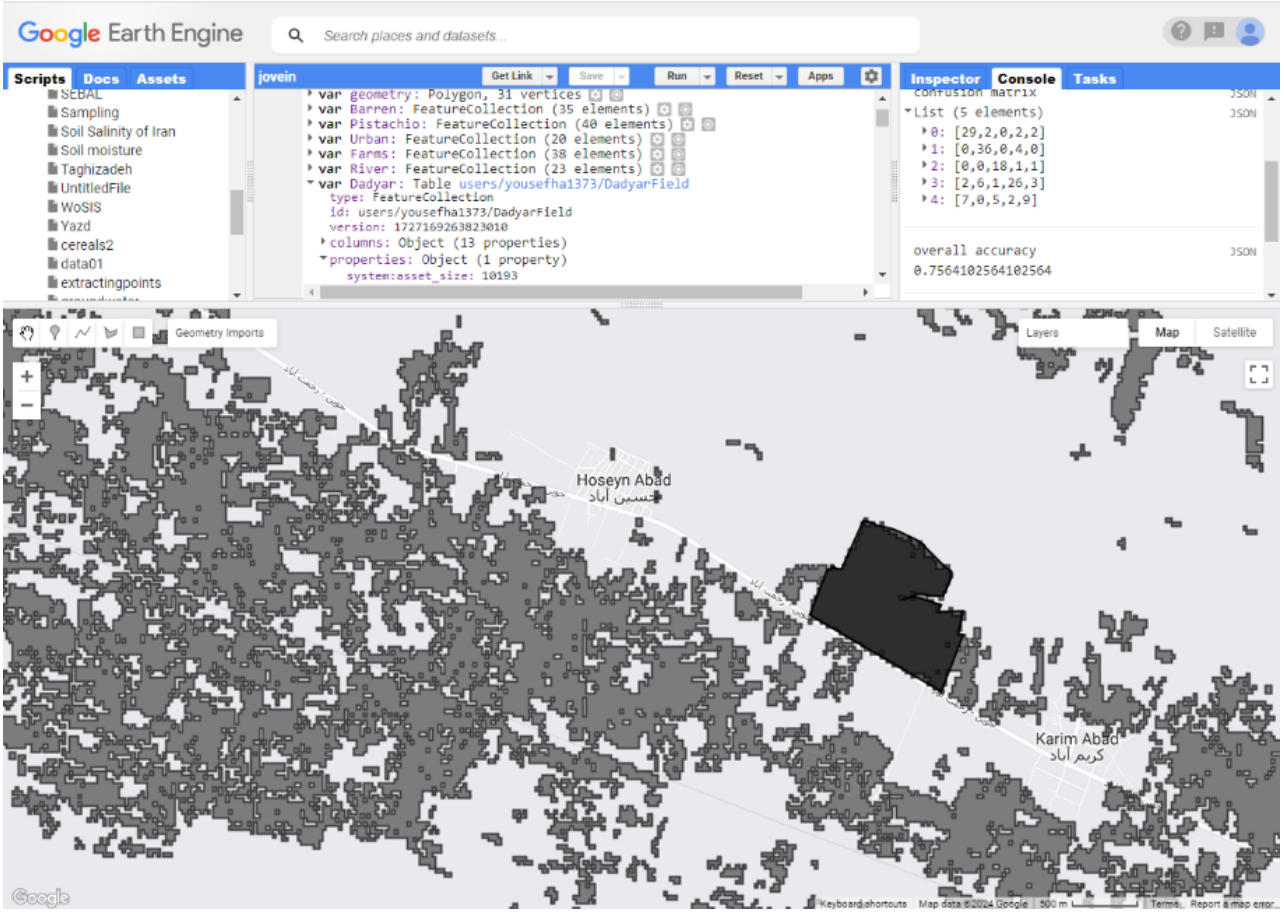

Figure 10. Boundary delineation of the studied orchard using the machine learning method in GEE.

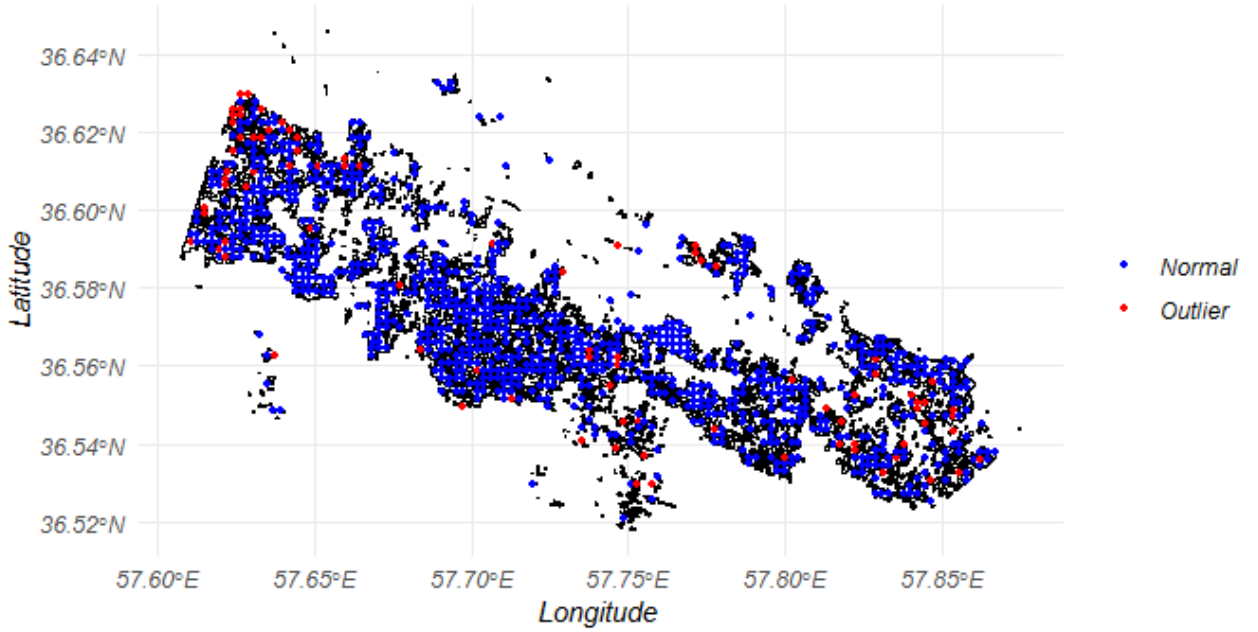

Figure 11. Regular sampling grid for extracting values of remote sensing variables.

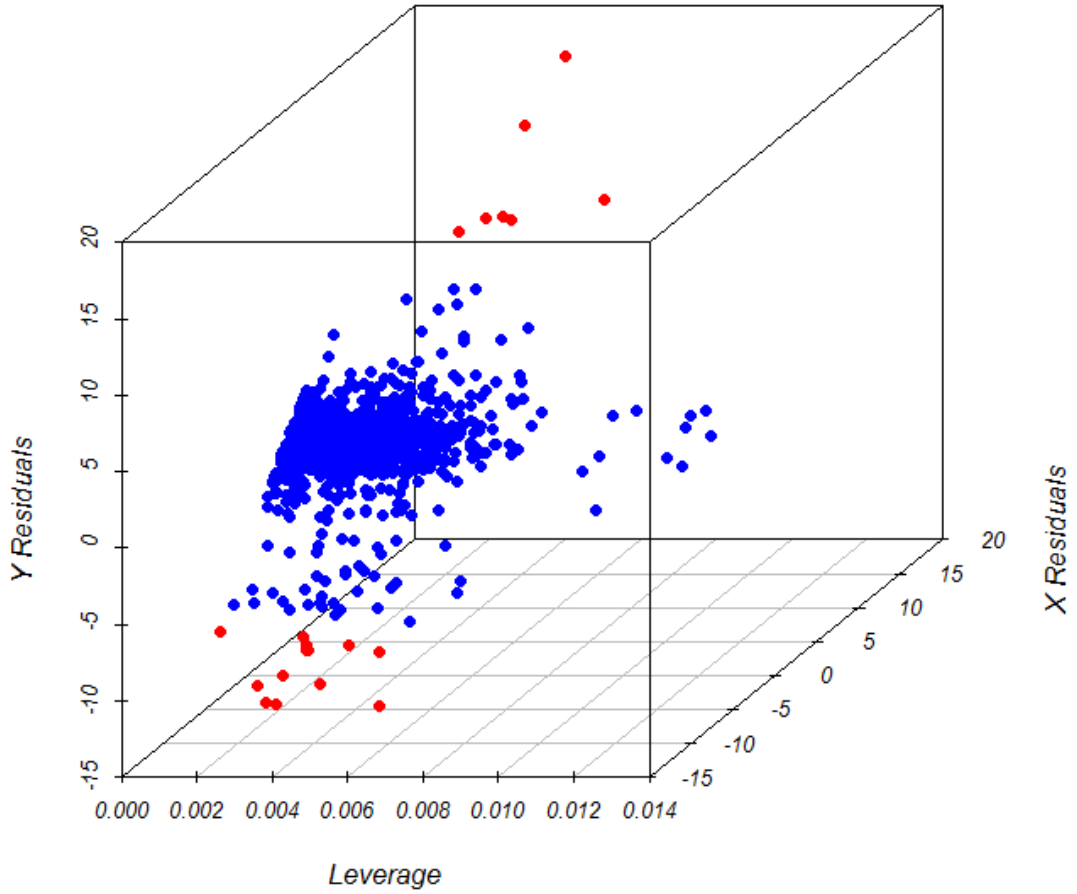

Figure 12. Detection of outliers using residual and leverage values.

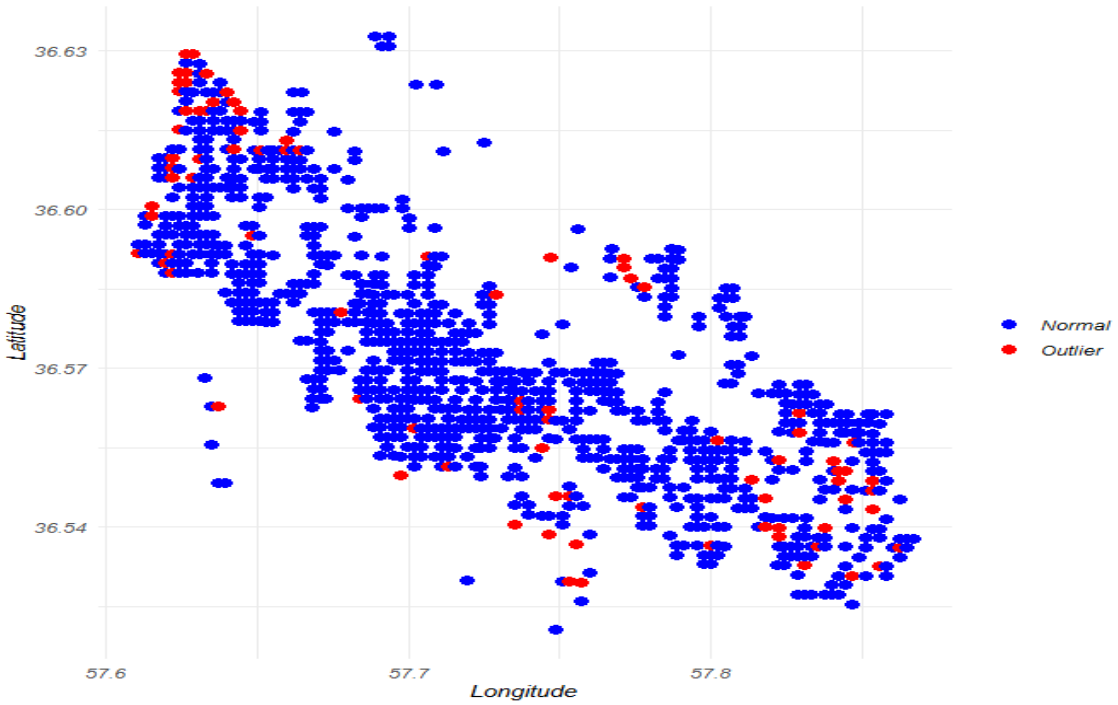

Figure 13. Location of outliers in the sampling points for remote sensing variables.

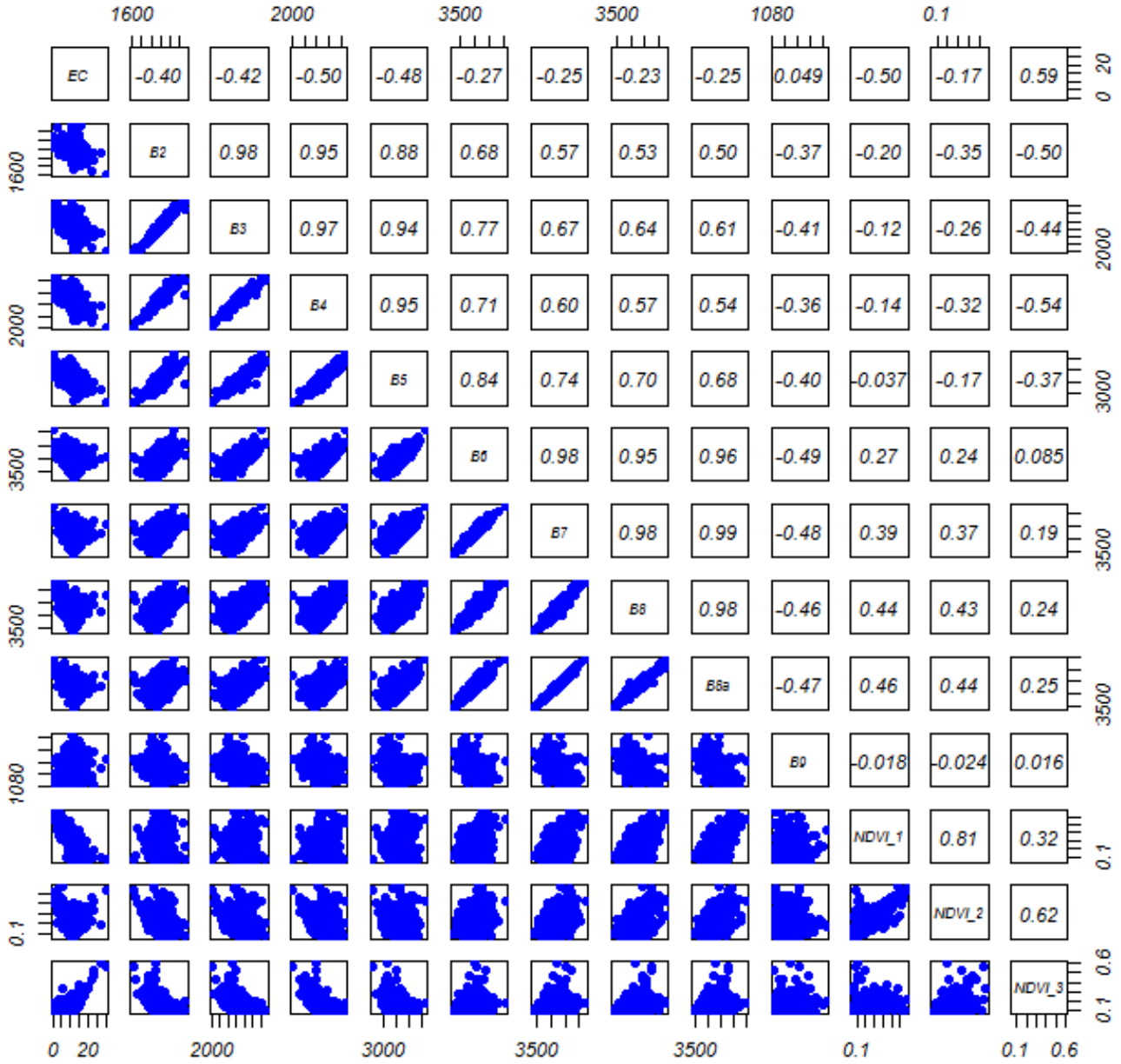

Figure 14. Correlation matrix between the variables used.

Aksoy et al. (2022) reported that by using various machine learning algorithms on the GEE platform and integrating them with indices derived from satellite images, they were able to monitor soil salinity changes along the margins of Lake Urmia.

4. Conclusion

This study demonstrated the potential of using remote sensing (RS) and proximal sensing (PS) indicators for modeling and mapping soil salinity in pistachio orchards irrigated with saline water. Although the relationships between predicted and observed soil salinity were statistically significant ($P < 0.01$), the coefficients of determination (R^2) ranged from 0.26 to 0.56, indicating only moderate predictive accuracy across the models. The integration of RS and PS indicators slightly improved model performance compared to using either dataset alone. Partial Least Squares Regression (PLSR) based on remote sensing indices was successfully applied to upscale salinity predictions over a 4080-hectare area using a combination of R and the Google Earth Engine (GEE).

Among the modeling techniques tested, the Support Vector Machine (SVM) method provided the highest accuracy, with an R^2 of 0.90 and a Root Mean Square Error (RMSE) of 0.75 dS/m, making it the most effective

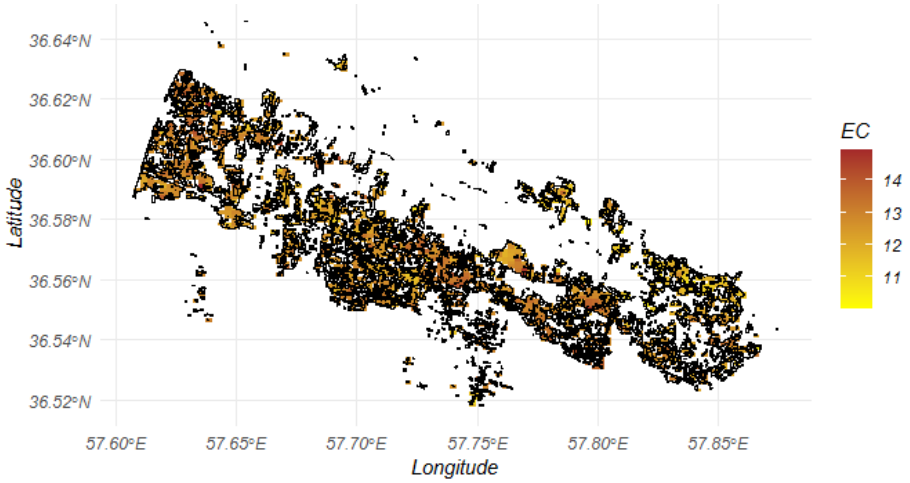

Figure 15. Soil salinity interpolation using IDW

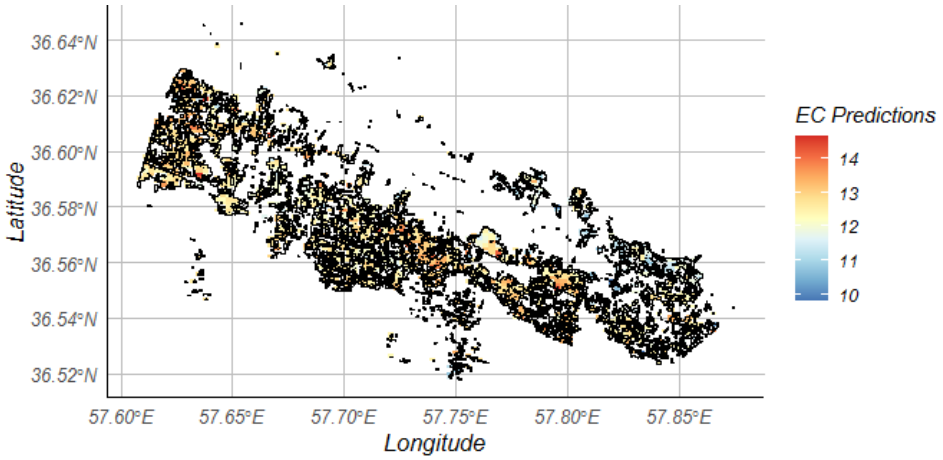

Figure 16. Soil salinity interpolation using RK

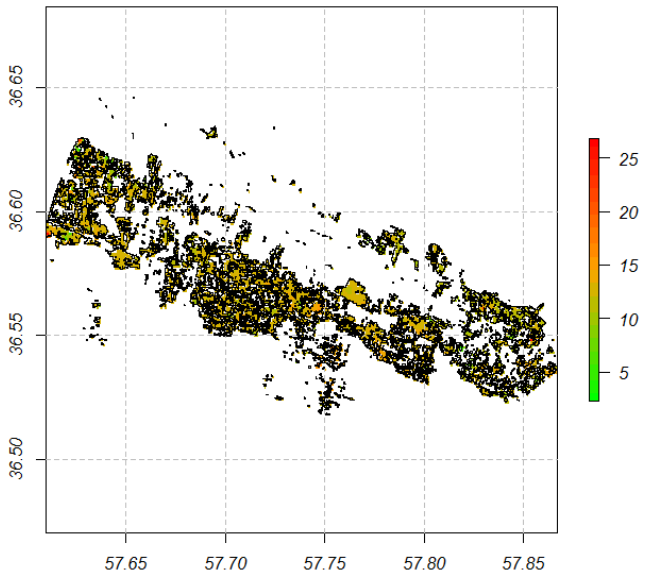

Figure 17. Soil salinity interpolation using support vector machine.

Table 5. Accuracy assessment of the three methods used for soil salinity interpolation.

Interpolaton Method	RMSE (dS/m)	MAE (dS/m)	R^2
IDW	1.11	0.86	0.48
RK	1.16	0.9	0.007
SVM	0.75	0.19	0.90

approach for generating a spatially detailed salinity map. Despite the moderate predictive power at the field scale, the integration of RS data offers a promising solution for regional salinity monitoring, particularly where ground-based measurements are limited. Future studies should aim to improve prediction accuracy by incorporating additional environmental covariates, higher-resolution data, and more extensive field validation to better capture the spatial heterogeneity of soil salinity.

References

Aksoy, S., Yildirim, A., Gorji, T., Hamzehpour, N., Tanik, A., and Sertel, E. (2022). Assessing the performance of machine learning algorithms for soil salinity mapping in Google Earth Engine platform using Sentinel-2A and Landsat-8 OLI data. Advances in Space Research, 69(2), 1072-1086.

Allbed, A., and Kumar, L. (2013). Soil salinity mapping and monitoring in arid and semi-arid regions using remote sensing technology: a review. Advances in remote sensing. 2(4), 373–385.

Brunner, P. H. T. L., Li, H. T., Kinzelbach, W., and Li, W. P. (2007). Generating soil electrical conductivity maps at regional level by integrating measurements on the ground and remote sensing data. International Journal of Remote Sensing, 28(15), 3341-3361.

Corwin, D. L., and Scudiero, E. (2019). Review of soil salinity assessment for agriculture across multiple scales using proximal and/or remote sensors. Advances in agronomy, 158, 1-130.

Delavar, M. A., Naderi, A., Ghorbani, Y., Mehrpouyan, A., and Bakhshi, A. (2020). Soil salinity mapping by remote sensing south of Urmia Lake, Iran. Geoderma Regional, 22, e00317.

Dong, W., Wu, T., Luo, J., Sun, Y., and Xia, L. (2019). Land parcel-based digital soil mapping of soil nutrient properties in an alluvial-diluvia plain agricultural area in China. Geoderma, 340, 234-248.

Fourati, T.H., Bouaziz, M., Benzina, M., and Bouaziz, S. (2017). Detection of terrain indices related to soil salinity and mapping salt-affected soils using remote sensing and geostatistical techniques. Environmental monitoring and assessment, 189, 1-11.

Gao, J., Zhao, Q., Chang, D., Ndayisenga, F., and Yu, Z. (2022). Assessing the effect of physicochemical properties of saline and sodic soil on soil microbial communities. Agriculture, 12(6), 782.

Ghassemi, F., Jakeman, A. J., and Nix, H. A. (1995). Salinisation of land and water resources: human causes, extent, management and case studies: CAB international.

Haq, Y. U., Shahbaz, M., Asif, H. S., Al-Laith, A., and Alsabban, W. H. (2023). Spatial mapping of soil salinity using machine learning and remote sensing in Kot Addu, Pakistan. Sustainability, 15(17), 12943.

Hassani, A., Azapagic, A., and Shokri, N. (2020). Predicting long-term dynamics of soil salinity and sodicity on a global scale. Proceedings of the National Academy of Sciences, 117(52), 33017-33027.

Iyer, G. R. S., Wang, J., Wells, G., Guruvenket, S., Payne, S., Bradley, M., and Borondics, F. (2014). Large-area, freestanding, single-layer graphene–gold: a hybrid plasmonic nanostructure. ACS nano, 8(6), 6353-6362.

Khorsandi, F., J. Vaziri and A. Azizi Zohan. (2010). Haloculture, sustainable use of saline water and soils in Agriculture. Iranian National Committee of Irrigation and Drainage. 320 pp. (in Persian).

Lagacherie, P., Arrouays, D., Bourennane, H., Gomez, C., and Nkuba-Kasanda, L. (2020). Analysing the impact of soil spatial sampling on the performances of Digital Soil Mapping models and their evaluation: A numerical experiment on Quantile Random Forest using clay contents obtained from Vis-NIR-SWIR hyperspectral imagery. Geoderma, 375, 114503.

Marino, G., Zaccaria D., Snyder RL., Lagos O., Lampinen BD., Ferguson L., Grattan SR., Little C., Shapiro K., Maskey ML., Corwin DL. (2019). Actual evapotranspiration and tree performance of mature micro-irrigated pistachio orchards grown on saline-sodic soils in the San Joaquin Valley of California. Agriculture, 9(4), 76.

Moameni, A. (2010). Geographical distribution and extent of saline soils in Iran. Soil Research. 24(3): 203-216.

Muhetaer, N., Nurmemet, I., Abulaiti, A., Xiao, S., and Zhao, J. (2022). A quantifying approach to soil salinity based on a radar feature space model using ALOS PALSAR-2 data. Remote Sensing, 14(2), 363.

Peng, J., Biswas, A., Jiang, Q., Zhao, R., Hu, J., Hu, B., and Shi, Z. (2019). Estimating soil salinity from remote sensing and terrain data in southern Xinjiang Province, China. Geoderma, 337, 1309-1319.

Rahimian, M. H., Shayannejad, M., Eslamian, S., Gheysari, M., and Jafari, R. (2019). Daily and Seasonal Pistachio Evapotranspiration in Saline Condition: Comparison of Satellite-Based and

Ground-Based Results. *Journal of the Indian Society of Remote Sensing*, *47*, 777-787.

Ren, D., Wei, B., Xu, X., Engel, B., Li, G., Huang, Q., Xiong, Y. and Huang, G. (2019). Analyzing spatiotemporal characteristics of soil salinity in arid irrigated agro-ecosystems using integrated approaches. Geoderma, 356, 113935.

Scudiero, E., Skaggs, T. H., and Corwin, D. L. (2014). Regional scale soil salinity evaluation using Landsat 7, western San Joaquin Valley, California, USA. Geoderma Regional, 2, 82-90.

Shamsi, S., Kamali, A., and Hasheminejhad, Y. (2022). An approach to predict soil salinity changes in irrigated pistachio orchards (Ardakan, Yazd Province): A case study. Journal of Soil Science Society of Iran, 1(1), 1-10.

Taghizadeh-Mehrjardi, R., Ayoubi, S., Namazi, Z., Malone, B. P., Zolfaghari, A. A., and Sadrabadi, F. R. (2016). Prediction of soil surface salinity in arid region of central Iran using auxiliary variables and genetic programming. Arid Land Research and Management, 30(1), 49-64.

Taghizadeh-Mehrjardi, R., Minasny, B., Sarmadian, F., and Malone, B. P. (2014). Digital mapping of soil salinity in Ardakan region, central Iran. Geoderma, 213, 15-28.

Taghizadeh-Mehrjardi, R., Schmidt, K., Toomanian, N., Heung, B., Behrens, T., Mosavi, A., Band, S.S., Amirian-Chakan, A., Fathabadi, A. and Scholten, T. (2021). Improving the spatial prediction of soil salinity in arid regions using wavelet transformation and support vector regression models. Geoderma, 383, 114793.

Tavares, S. R., Vasques, G. M., Oliveira, R. P., Dantas, M. M., and Rodrigues, H. M. (2024). Random Forest-Based Fusion of Proximal and Orbital Remote Sensor Data for Soil Salinity Mapping in a Brazilian Semi-arid Region. In: Pedometrics in Brazil (pp. 197-209). Cham: Springer Nature Switzerland.

Wang, F., Yang, S., Wei, Y., Shi, Q., and Ding, J. (2021). Characterizing soil salinity at multiple depth using electromagnetic induction and remote sensing data with random forests: A case study in Tarim River Basin of southern Xinjiang, China. Science of the Total Environment, 754, 142030.

Wang, J., Ding, J., Abulimiti, A., and Cai, L. (2018). Quantitative estimation of soil salinity by means of different modeling methods and visible-near infrared (VIS–NIR) spectroscopy, Ebinur Lake Wetland, Northwest China. PeerJ, 6, e4703.

Wang, N., Chen, S., Huang, J., Frappart, F., Taghizadeh, R., Zhang, X., Wigneron, J.P., Xue, J., Xiao, Y., Peng, J. and Shi, Z. (2024). Global Soil Salinity Estimation at 10 m Using Multi-Source Remote Sensing. Journal of Remote Sensing, 4, 0130.

Xiao, C., Ji, Q., Chen, J., Zhang, F., Li, Y., Fan, J., Hou, X., Yan, F. and Wang, H. (2023). Prediction of soil salinity parameters using machine learning models in an arid region of northwest China. Computers and Electronics in Agriculture, 204, 107512.

Yimer, A. M., Sodango, T. H., and Assefa, S. A. (2022). Analysis and Modeling of Soil Salinity Using Sentinel-2A and LANDSAT-8 images in the Afambo Irrigated Area, Afar Region, Ethiopia. Preprints. https://doi.org/10.20944/preprints202204.0250.v1

Zare, S., Abtahi, A., Shamsi, S. R. F., and Lagacherie, P. (2021). Combining laboratory measurements and proximal soil sensing data in digital soil mapping approaches. Catena, 207, 105702.

Zhao, S., Ayoubi, S., Mousavi, S.R., Mireei, S.A., Shahpouri, F., Wu, S.X., Chen, C.B., Zhao, Z.Y. and Tian, C.Y. (2024). Integrating proximal soil sensing data and environmental variables to enhance the prediction accuracy for soil salinity and sodicity in a region of Xinjiang Province, China. Journal of Environmental Management, 364, 121311.